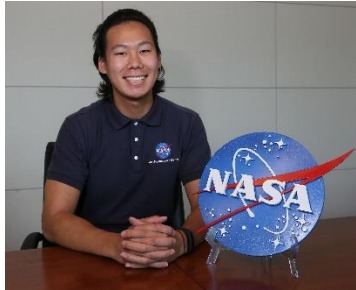


# **An Elegant and Innovative Design for In-Space Assembly: Optimizing Modularity through an Umbrella Mechanism**

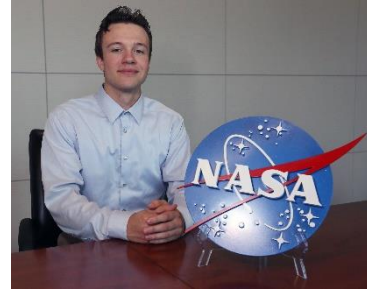
NASA BIG Idea Challenge  
Technical Report, February 7, 2017



Zachary Bassett  
Senior Undergraduate Student  
University of Texas at Austin  
Aerospace Engineering

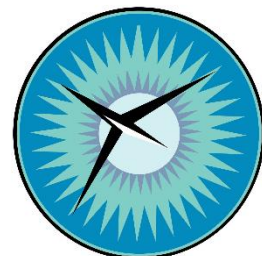
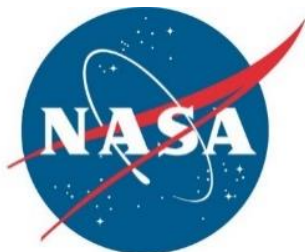


Henry Kwan  
First Year Graduate Student  
Georgia Institute of Technology  
Mechanical Engineering



Peter Finch  
Senior Undergraduate Student  
New York University Poly.  
Mechanical Engineering

Advisor: Dr. Daniel Schrage  
Professor & Director CERT & CASA  
Georgia Institute of Technology  
School of Aerospace Engineering



## I. INTRODUCTION

The need for space systems that have the capability to be assembled in space and re-used for additional missions is essential in reducing the cost of deep space exploration. Through the use of autonomous robotics, space system components can be assembled in space without human interaction. Space system components can be accumulated in one location (or multiple launches) and then assembled in space. In-space assembly allows for space system components to be efficiently stored in launch vehicles, launched into appropriate orbits, and assembled in-space for a functional spacecraft. The modularity of the components of the spacecraft allow for easier repairs, upgrades, and reconfiguration of spacecraft to better fit another mission.

NASA's evolvable mars campaign (EMC) is planning to use a LDRO to stage space systems for various missions ranging from lunar excursions, asteroid rendezvous, and Mars exploration by humans. With recent advances in electric propulsion and efficiency of solar arrays to generate power, space systems can be moved at a much lower cost and risk than using chemical or nuclear propulsion. Solar electric propulsion (SEP) modules are needed in order to transfer large space systems between LEO and LDRO with power requirements of 200 kW with expendability to 500 kW [1].

Spacecraft are currently fully integrated on Earth with all of the subsystems and spacecraft structure attached to the launch vehicle. Once the launch vehicle reaches the spacecraft separates and deploys into its functional configuration. This approach has the advantage of being able to conduct a full systems check of the spacecraft before launch, however the spacecraft undergoes heavy loads during launch which could cause failure. The launch vehicle has limited volume which is defined by the vehicle fairing size. The assembly of a 200 kW or larger SEP with this current approach would cause a very complex packaging and deployment process, the need for an in-space assembly process is crucial.

## II. LITERATURE REVIEW

This section provides a summary of the information found in the literature to develop the Concept of Operations (CONOPs) proposed. The main systems required include an orbital launch system, solar arrays, electric propulsion, and robotics. The literature review analyzed the technologies in each field that showed the most potential in supporting the given mission requirements as shown in Table 1.

**Table 1.** System Technologies

Name	Type	Specifications
Falcon 9	Orbital Launch System	Cost: \$61.1 million Mass to LEO: 13,150 kg Fairing Diameter: 5.2 m Fairing Length: 14.3 m Fairing Mass: 1,750 kg
Orbital ATK MegaFlex	Solar Arrays	Mass: 1250 kg Power: 200kW
NASA Evolutionary Xenon Thruster	Electric Propulsion	Mass: 4.8 kg/kW Power Range: 0.5-6.9 kW Propellant: 300 kg Max Specific Impulse: 4190 s Thrust: 236 mN
Canadarm2	Robotics	Mass: 225 kg Peak Power: 2 kW Average Power: 0.4 kW
Electro Permanent Magnet	Robotics	Mass: 10 kg Power: 2 kW

The Falcon 9 was selected as the orbital launch system based off the mission requirement that the rocket must be able to carry a ~10,000 kg payload to LEO [2]. The review looked at rockets currently in use and the selection was based on the launch cost, payload mass to LEO, success rate, and payload fairing dimensions. The Space Launch System (SLS) was not taken into consideration since it is still in development and the launch cost would outweigh the costs of using smaller rockets. In addition, SLS is not within the scope of this challenge, as the mission is to launch several smaller rockets rather than one large rocket. Other alternative options for a rocket could include the Atlas V and Delta IV since the launch cost and payload fairing dimensions are also relatively similar to the Falcon 9. The European Space Agency's (ESA) Ariane 6, currently in development, might also be a competitor to the Falcon 9 in the near future.

The Orbital ATK MegaFlex was selected as the solar array system. The MegaFlex Advanced Solar Array for SEP is at a high TRL maturity and is scalable up to 500 kW [3]. This satisfies the mission requirements. Given the Falcon 9 as the orbital launch system, the MegaFlex meets the payload fairing dimensions. In addition, the ATK MegaFlex can withstand up to 3G load satisfying the mission requirement of 0.4G [3]. The MegaFlex performance vs. diameter metrics shown in Figure 1 was used to partially derive the specifications of the MegaFlex system shown in Table 1 that will be used for the system.

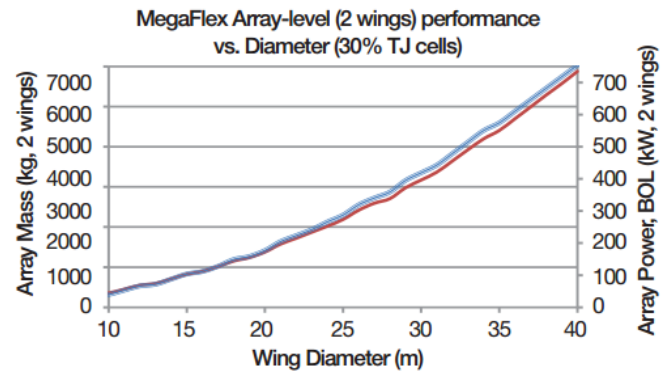


**Figure 1.** ATK MegaFlex Performance v. Diameter [3]

The success of the mission is dependent on the application of Solar Electrical Propulsion to bring the payload from LEO to LDRO. Trade studies have been performed for the current available thrusters and their TRL. NASA Evolutionary Xenon Thruster (NEXT) has been under investigation for the last decade at the Glenn Research Center and has completed a 5 year trial for system performance [4]. The NEXT has also been in used in an array configuration, with power and thrust values scaling linearly with no observed interfering interactions. NEXT is slated to be ready for interplanetary missions as part of the New Frontiers missions by the 2019 time frame [5]. As such, its TRL is high and can be used as a suitable benchmark for the scaling of the SEP on board this vehicle. Additionally, other Hall Thrusters were investigated to serve as a justification for the benchmark feasibility of NEXT. One such study was a 6 kW Hall Thruster developed by the Airforce, JPL, and the University of Michigan with an Isp of 2000s and 397 mN peak thrust [6].

Robotics such as the Canadarm2 Mobile Servicing System are currently being used on the International Space Station (ISS) to service payloads and instruments attached and assist astronauts or autonomously transport supplies and equipment around ISS [7][8]. Robotic arms have also been used on NASA missions such as the DARPA Orbital Express Mission which relied on a robotic arm to grab and dock two satellites together [9]. It is also good to note that for most of the approach, the long range rendezvous, optical and infrared imaging sensors were used [9]. In addition, the robotic arm was able to transfer commodities across the two satellites. However, one area made the mission short of being fully autonomous, which was the aligning of the two satellites by a ground controller for final docking. A similar robotic servicing mission currently in development that will perform the same functions proven in the Orbital Express mission is the NASA Restore-L [10].

Magnets have been discussed heavily in the space industry as it operates perfectly in a vacuum is independent of a medium. Recent advances in technologies has introduced a new alternative to electromagnets; the Electro-Permanent Magnet (EPM). Whereas electromagnets consume large amounts of energy while operating, EPMs require no power source to maintain the magnetic field [11]. A small electric pulse is all that is required to make an EPM permanent, in a state of attraction, and another pulse to remove the magnetic force. An electro-permanent magnet (EPM) houses two sets of magnets connected by two iron cores. In the off-state, the magnetic flux is conducted from one set of magnets to the other through the cores.

Using the principles of induction and coercivity, a short electric pulse permanently reverses the polarity of one of these magnet sets, causing the two cores to become polarized and create a net attractive magnetic force [12].

### III. DESIGN

#### III.I Concept of Operations

To determine the number of launches that would be needed to take all of the components of the spacecraft into LEO; a simple figure of merit was done. The figure of merit can be seen in Table 2. From the figures of merit, it was found that the optimal number of launches would be two or three; normalized scores of 0.58 and 0.56 respectively. Due to volume requirements in the payload fairing, 3 launches using the Falcon 9 was chosen.

**Table 2.** Figures of Merit to Determine Number of Launches

Number of Launches	Cost of Launch	Complexity of Packaging	Complexity of Assembly	In-Space Assembly	Score
1.00	1.00	0.00	1.00	0.00	0.40
2.00	0.89	0.11	0.89	1.00	0.58
3.00	0.78	0.22	0.78	1.00	0.56
4.00	0.67	0.33	0.67	1.00	0.53
5.00	0.56	0.44	0.56	1.00	0.51
6.00	0.44	0.56	0.44	1.00	0.49
7.00	0.33	0.67	0.33	1.00	0.47
8.00	0.22	0.78	0.22	1.00	0.44
9.00	0.11	0.89	0.11	1.00	0.42
10.00	0.00	1.00	0.00	1.00	0.40

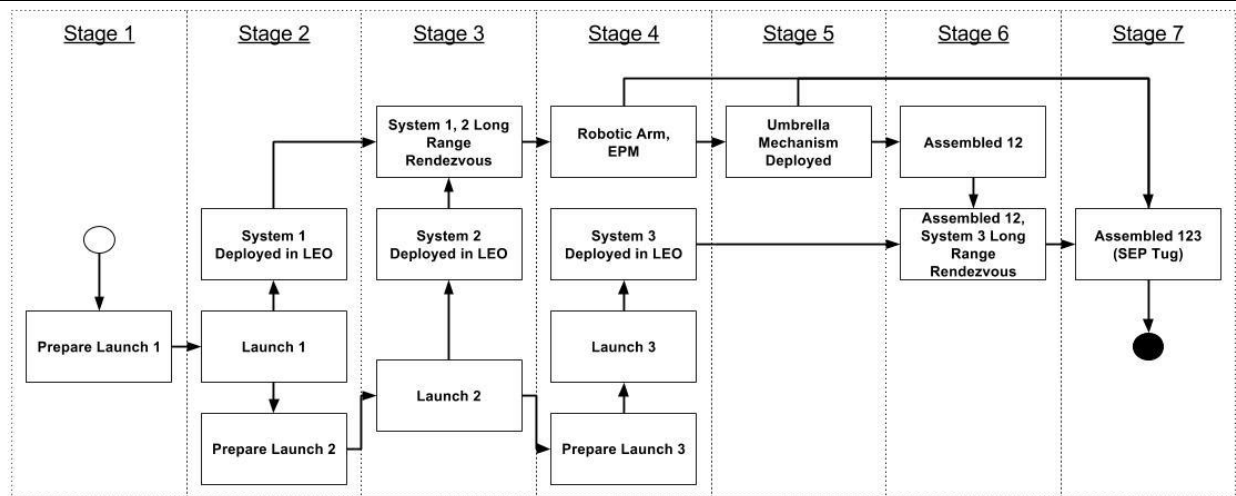


**Figure 2.** Sequence Diagram of Events from Launch to Assembly

Based on the FOM and dimensions of the payload fairing, the SEP Tug will be split into three modules. The first module will contain the solar arrays and robotics, the second module will contain the electric propulsion, and the third module will contain the tug and payload. These three modules will be stowed and packaged efficiently in the Falcon 9 payload fairing. A sequence diagram of the events is shown in Figure 2 and a Bat chart from ground to LDRO is shown Figure 3. There are seven stages from the point of the first launch to the final assembly of the SEP Tug. As shown in Figure 2, the sequence of events operate both in parallel and series. This operation ensures that the sequence of events operates efficiently. For

example, while the first module is launched and deployed in LEO, simultaneously the second module is being prepared for the second launch. The goal is to minimize the amount of time spent in LEO when the modules are separated.

Once in LEO the modules will be deployed and begin to operate fully autonomously. The modules will have an autonomous Orbital Express Rendezvous Guidance, Navigation, & Control (OERGNC) system that will achieve: autonomous guidance from 200 km rendezvous to capture, autonomous robotic free capture and positioning, autonomous attitude software points, autonomous internal checks and failure detection. The sensors on board include Narrow-Field-of-View and Wide-Field-of-View optical sensors, infrared sensors for night vision, and an independent laser-based imaging tracker that only activates during the final approach and capture of the modules. Based off the Orbital Express mission, the time it takes for the modules to rendezvous is 11 days for each rendezvous.

The solar arrays and robotic module will serve as the main body in which electric propulsion module will attach to, followed by the tug and payload module. On the end of the robotic arm is an EPM. Once the electric propulsion module is within range of the main body, the robotic arm will grab and capture the module via the EPM, and reorient the module to precisely align and the modules together for docking. Once the system detects there is a connection, an umbrella mechanism will be deployed which will complete the assembly of the modules. Once this is complete, the same process will occur with the last module. Given the simplicity of the robotic arm, EPM, and mechanism, the total time it will take for the modules to assemble is three days for each module.

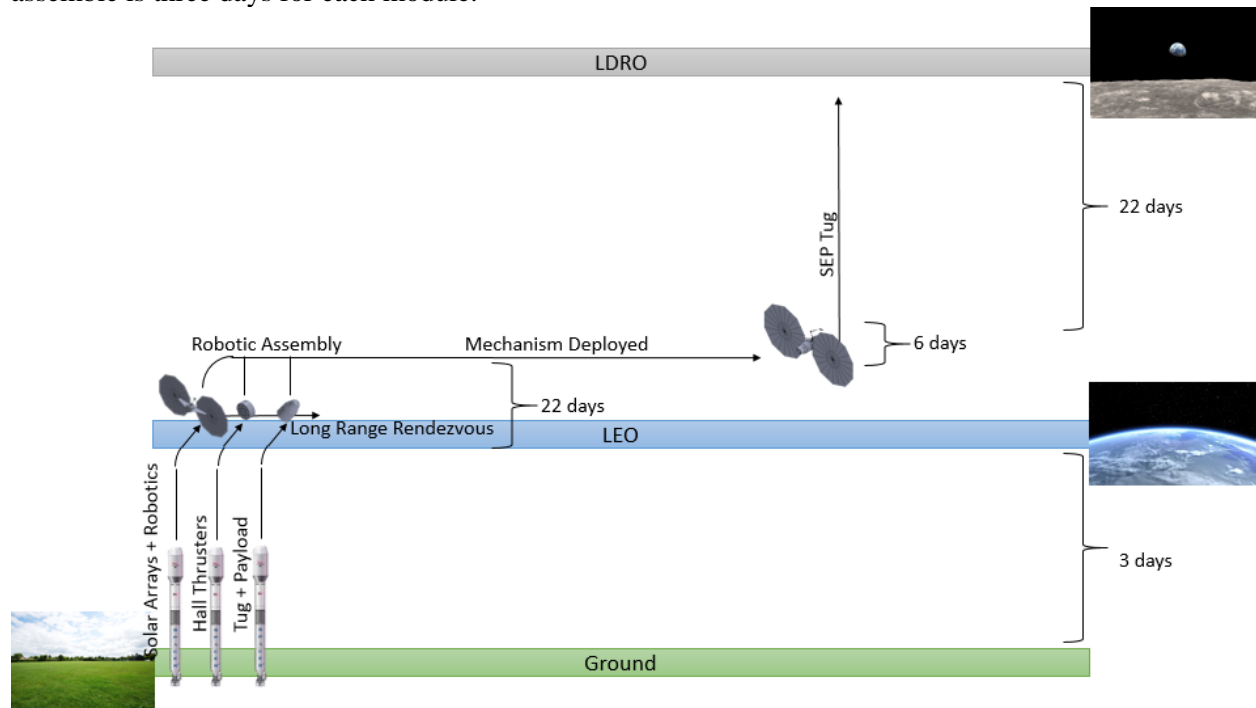


**Figure 3.** CONOPs - Ground to LEO to LDRO

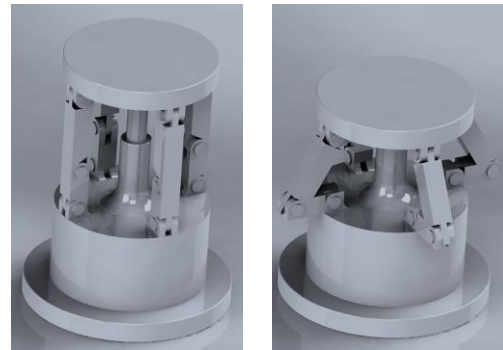
### III.II Umbrella Mechanism

As discussed in the CONOPs in the previous section, the umbrella mechanism is what finalizes the assembly and completely docks the modules together. As shown in Figure 4, the mechanism has two states; up and down. The up configuration is to allow the modules to connect and the down configuration fastens the two modules together. These states are controlled by a linear actuator in the center of the mechanism that has two modes, up and down, that controls the two states, respectively. Through many iterations, this

mechanism was designed based on its simplicity, feasibility, and mass. The simplistic design of the mechanism offers higher system reliability and removes additional modes of failure.

The electric propulsion and tug/payload modules will have the docking plates as shown in Figure 5. The docking plates will be the female end while the umbrella mechanism acts as the male ends. For each plate, there will be three umbrella mechanisms oriented in a circular pattern as shown in Figure 6. In addition, each module will have three plates, thus nine umbrella mechanisms will be used for each module. The selection amount was chosen to eliminate all translation and rotational movement.

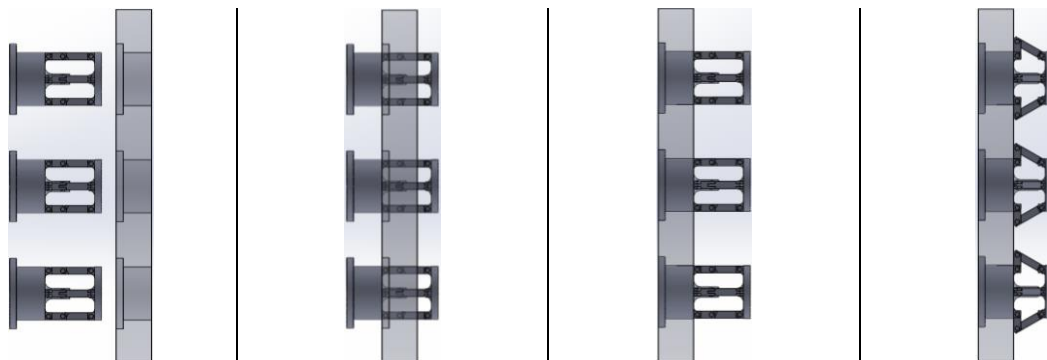
As shown in Figure 5, though the mechanism has two states, there are four stages for the modules to be completely assembled. Stage 1, alignment is achieved through the robotic arm, EPM, sensors, and onboard computer. Once the system detects accurate alignment, the male and female end will translate until they are flush. Once the system detects that the two modules are level, the mechanism will be deployed. The mechanism has the ability to unlatch and disassemble the modules allowing for modularity. This provides engineers the ability to replace or repair modules in future missions. For example, the mechanism can un-deploy, operating the four stages in reverse order, remove a module and rendezvous with a new module while the other is sent back for repair. The material selected for the umbrella mechanism was aluminum. Aluminum was selected due to the material properties of high strength and low density compared to other materials.



**State 1: Up**

**State 2: Down**

**Figure 4: Umbrella Mechanism Stages**



**Stage 1: Alignment**

**Stage 2: Translation**

**Stage 3: Level**

**Stage 4: Deployed**

**Figure 5. Side View - Stages of Mechanism Deployment**

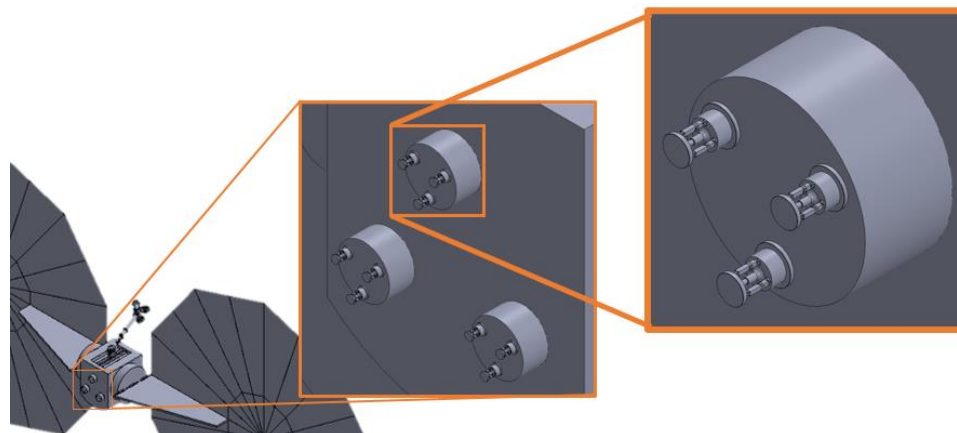


**Figure 6. Isometric Mechanism View from the Solar Arrays & Robotic Module (System 1)**

## IV. ANALYSIS

### IV.I Assembly

#### Launch and Unpacking

The spacecraft is brought to orbit in three separate launches aboard Falcon 9 rockets. The first launch will place the base module in LEO. This module consists of the robotic armature and the solar arrays to power the tug. The second launch provides the hall thruster module, consisting of 17 thrusters. In the future, if the system is scaled up or there are multiple tugs in continuous operation, multiple hall thruster modules can be brought to orbit in the same launch. The final launch is the payload itself. Subsequent launches can also include more payloads as the tug operates back and forth between LEO and LDRO. For the purposes of the presentation, a Dragon capsule is used as the payload. The three modules must be capable of fitting within the workable space of a Falcon 9 payload fairing. Renderings of the three different launch payloads are depicted in Figure 7 as section views cut through the fairing, exposing the inside. The greatest challenge to the packaging is the solar arrays, which have a diameter of 10 m. The ATK arrays are designed to not only fold up flat, but also fold back along the radius of the array. By positioning the assembly at an angle in the fairing, the entire module fits within the workable space.

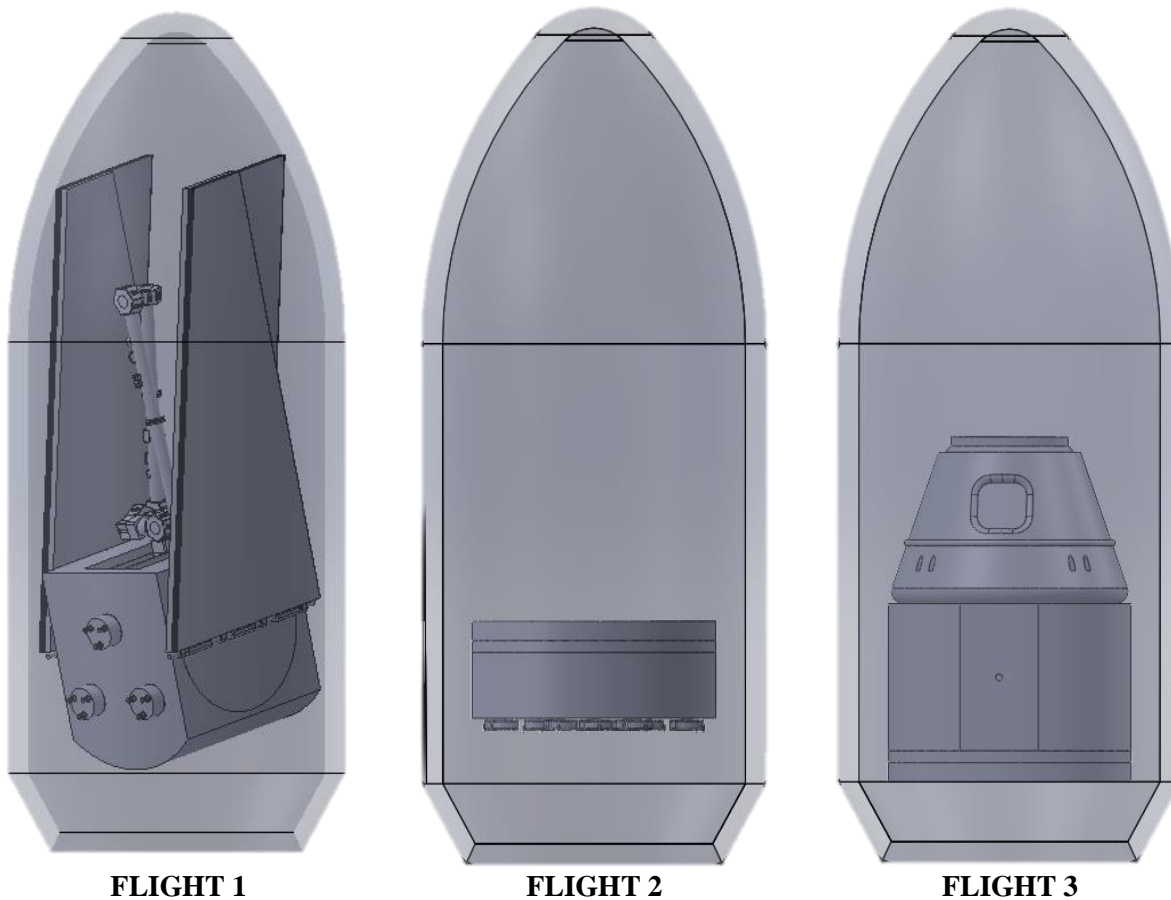


**Figure 7.** Side View of Modules Packaged (left: Base Module, middle: Hall Thruster Module, right: Payload and Tug Module)

Once in space and clear of the fairing, the modules must deploy. For the base module, the first step in this process is to fold forward the solar arrays so that all panels lay flat along the constant axis. The arrays themselves are hinged to the base module, allowing them to rotate along the axis of the spacecraft. Having rotated  $90^\circ$ , the arrays then open up around the supporting base. There is enough clearance for the arrays

to fully deploy without interfering with the base module. However, in order to clear space for the rest of the spacecraft, the arrays are advanced transverse to the axis of the spacecraft by linear actuators. Finally, these actuators themselves are held in a bearing assembly which can rotate about this transverse axis. As such, the solar arrays can be positioned to maximize incident solar radiation. With the arrays deployed, the tug can now enter its normal power regime. The robotic arm is now available for subsequent docking.

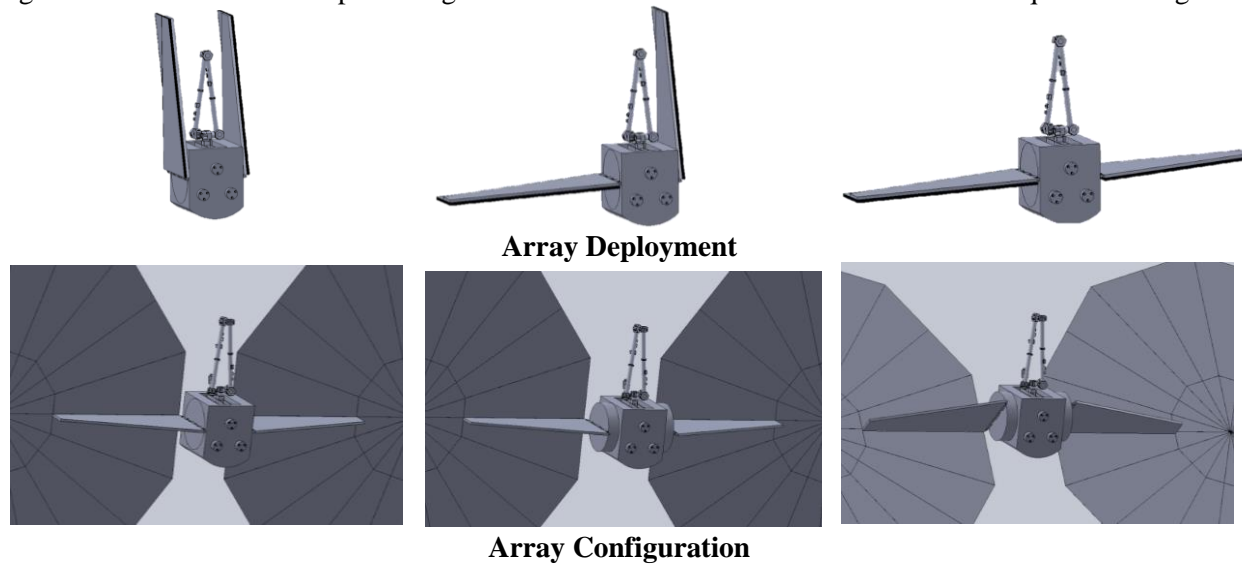


**Figure 8.** Solar Array Deployment Stages

### Robotic Arm

The robotic arm is a 7 DOF system consisting of two large booms and multiple joints. The system is constructed from high strength carbon fiber thermoplastic, weighing around 225 kg. Each joint is 1 DOF in rotation. The booms each project over 3.3 meters. At the base of each boom is an assemblage of three such joints, and there is one joint which articulates the booms about each other. The base of the arm lies on a track running 2.4 meters on the upper surface of the spacecraft, allowing for added motion in the axial direction. This adds to the overall reach radius of the arm during the docking procedure, should it be necessary.

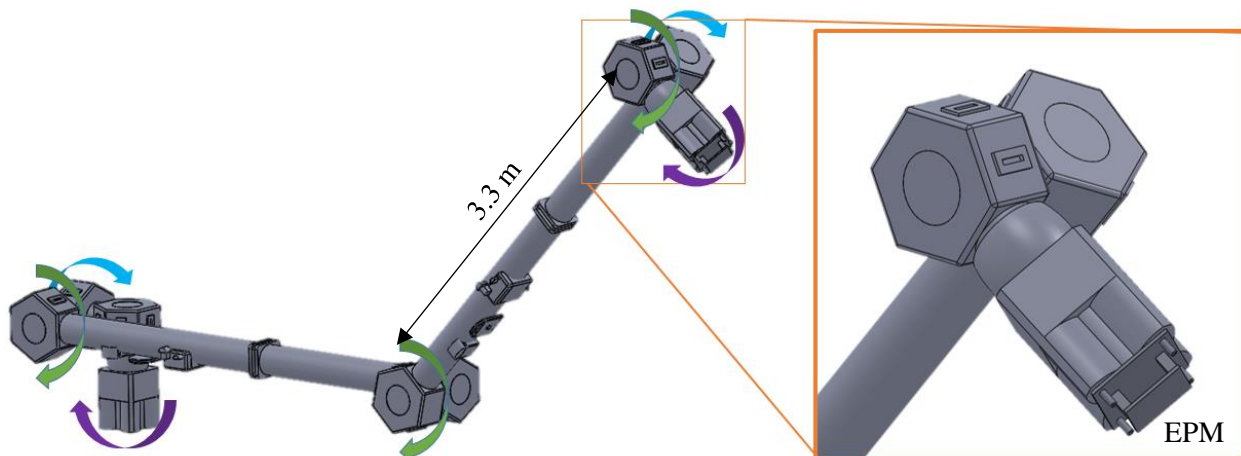


**Figure 9.** Arm Degrees of Freedom and EPM

The many degrees of freedom allow for a variety of configurations during the docking procedure. However, the redundancy in flexibility is desired given the many possible permutations of attitudinal and translational offset between docking modules. One such docking procedure is provided below. Once the

modules are flush, the umbrella mechanism serves as the final method of attachment and the arm is no longer needed.

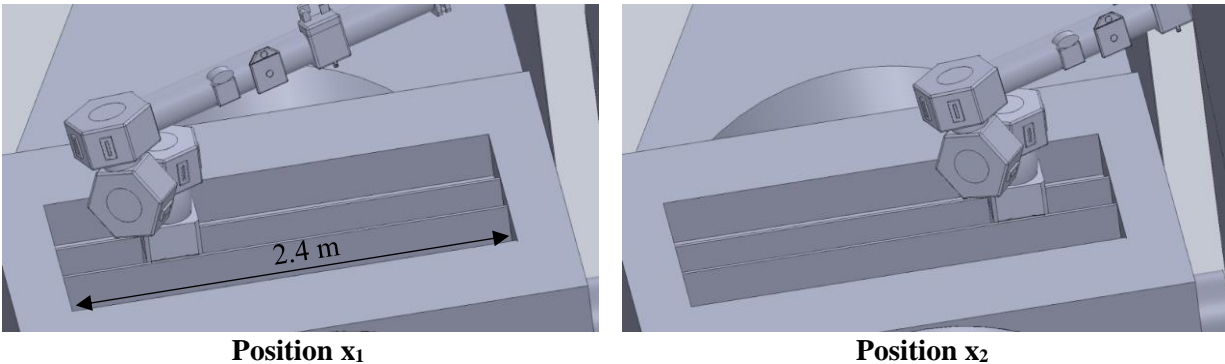


**Figure 10.** Arm on Track

At the end of the robotic arm is an Electro-Permanent Magnet (EPM), which serves as the grappling element during the docking process. The EPM can attach to any number of designated locations on the surface of the secondary module. The robotic arm and EPM in operation draw no more than 2 kW, well within the allotted power budget. When not in use, the arm draws minimal power and the EPM draws none.

#### Propulsion Module.

The propulsion for LEO to LDRO transit is provided by 17 Hall Thrusters laid out in a radially and rectangularly symmetric configuration to not create any adverse moments. This configuration is two concentric circles of 8 thrusters offset by 45°. The thrusters are NASA's Evolutionary Xenon Thruster, and each draws 6.9 kW. The entire assembly of thrusters draws a little more than half of the available power of the arrays, necessitating the latter's deployment first. The propulsion module does not require any mechanical actuation to deploy; it is ready for operation after jettisoning the fairing. The forward face is equipped with the female end of the umbrella mechanism

#### SEP Tug

The same docking procedure is employed for the payload and tug module. The spacecraft is thus complete after two docking procedures. The spacecraft is laid out with the payload section up front, the base module with the articulating solar arrays and arm in the middle, and the hall thruster module in the rear. As stated, a standard Dragon Capsule is being used as the payload in this report, but any such payload is possible so long as the tug is similarly equipped with its own female end to the umbrella mechanism.

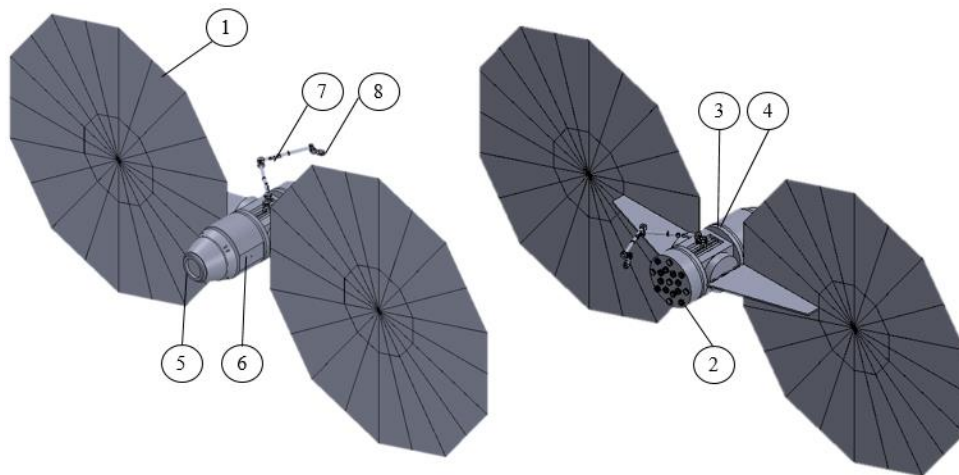


**Figure 11.** Spacecraft Ready for Lunar Trajectory

No.	Component	Mass (kg)	Qty.	No.	Component	Mass (kg)	Qty.
1	Solar Array	625	2	5	Tug	500	1
2	Hall Thruster	33.1	17	6	Payload	3500	1
3	Umbrella Mechanism	0.91	18	7	Robotic Arm	225	1
4	Docking Plate	5.0	6	8	EPM	2.5	1

**IV.II Numerical Analysis**

Finite Element Analysis

As the method for final attachment between modules, the umbrella mechanism must be able to withstand loads associated with the acceleration and deceleration of the spacecraft. Since accelerations in the positive direction (along the thrusting vector of the hall thrusters) bring the respective plates of the modules into contact, it is these broad surfaces that bear the load. Therefore, it is of critical importance to test relative motion in the opposite direction, one that tends to draw the modules apart and compress the umbrella mechanism. Finite Element Analysis was thus performed to certify the strength and soundness of the umbrella mechanism.

To do so, one mechanism was tested individually. For each contacting surface, there are three sets of three mechanisms (a total of nine). Moreover, to reduce the computational cost of the simulation, the mechanism itself was divided on symmetry planes into quarters. As such, only 1/36th of the total load-bearing surface was applied. Each piece of the mechanism was meshed independently. Patch conforming methodology was preferred given the preponderance of curved surfaces. Inflation was used around where the hinges on the assembly, where the vast majority of the stress was expected to be borne.



**Figure 12.** Meshing

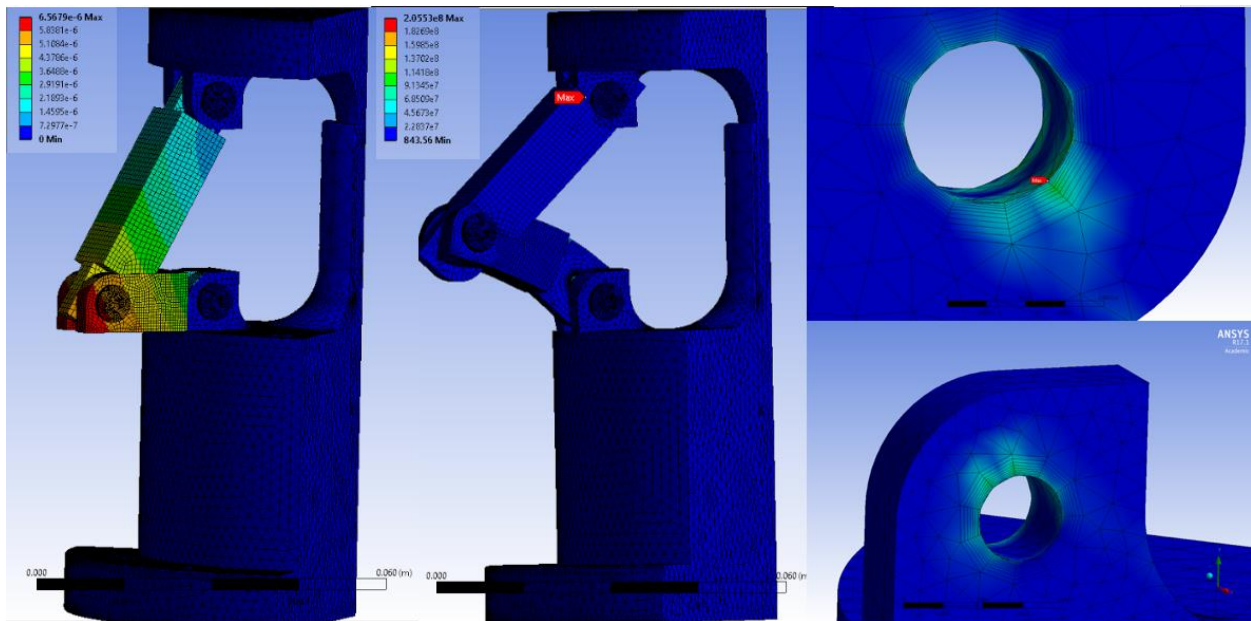


**Figure 13.** Left: Displacement, Center: Stress with displacement magnified 2400x, Right: Max Stress on hole and supports

The system was constrained at the base, where it would be attached to the spacecraft. Additionally, the linear actuation shaft was bonded, as this would be electromagnetically fixed. All holds and surfaces were constrained using a frictional contact condition. A load of 500 N was applied on the shorter arm in an upward direction. In Figure 13, some results are depicted. The displacement is shown on the left of the image. In the center, the displacement is exaggerated by 2400x to demonstrate the method of strain. On the right, the maximum stress is depicted, as well as the stress on one of the pins.

The resulting simulation demonstrated the majority of the stress focused on the pin holes. The vast majority of the structure experienced limited stress. Stress was maximized at approximately 205 MPa, with displacements of only about 10 microns experienced locally. Various treatments of Aluminum 6061 have yield strengths greater than 300 MPa. Additionally, reinforcements can be provided to support even larger loading. With an equivalent loading of 18000 N satisfied with factors of safety, the spaceship is capable of handling 0.4 G's of acceleration based on current mass buildup.

### Arm Testing

It is important that the robotic arm also be capable of surviving under stressors. More Finite Element Analyses were performed on the arm under load. To perform such analyses, the booms were extended fully to maximize the moment arm. Bearing loading constraints were applied on all the shafts. Multiple analyses were conducted, some with the joints bonded, others with them free to rotate. Naturally, the bonded trials yielded largest stresses in the structure. In actuality, the armatures great flexibility makes it resistant to stresses, as any configuration that bends the booms can be remedied by rotating the armature about one of its joints. In this fashion, modules can be accelerated slowly with a small application of force and limited strain on the structure. Even still, with 5000 N of load applied at the maximum extent of the structure (6.6 m away from the base) and all joints fixed, the maximum von-Mises stress is 68 MPa experienced mainly as bending stress in the booms. This is well within the linear elastic region and not a concern of failing.

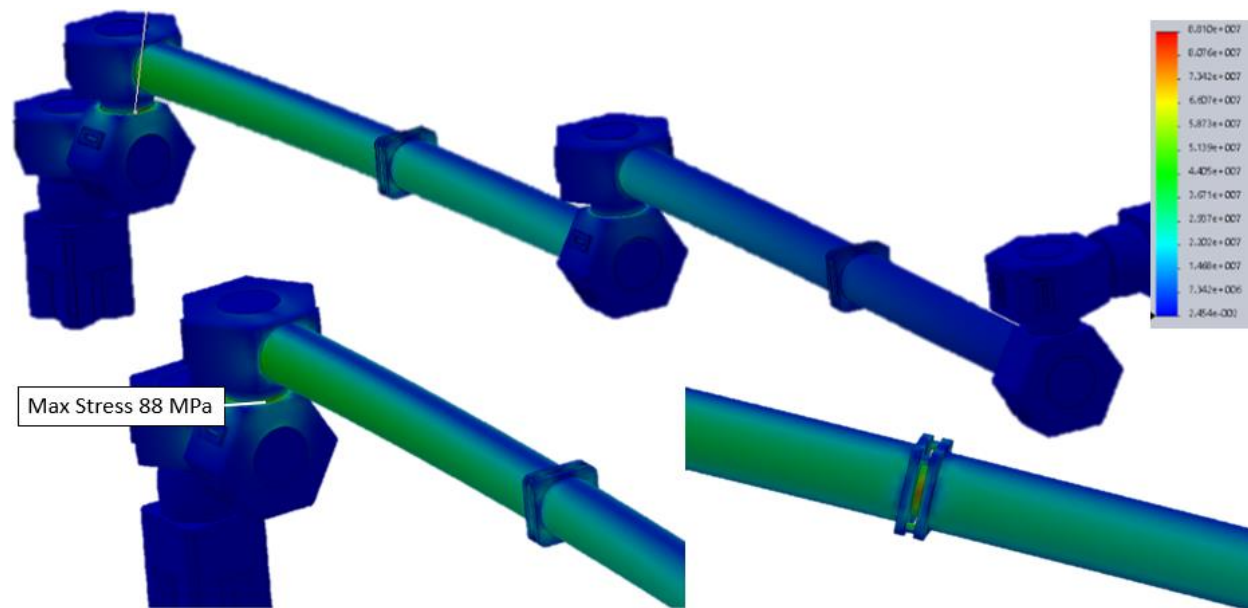


**Figure 14.** FEA on the Robotic Arm, Stress in Pa

### Modal Analysis

Competition requirements stipulate a 0.05 Hz fundamental frequency floor. Modal analysis in FEA was performed to ensure all launching modules satisfy this requirement. The Orbital ATK MegaFlex arrays have a fundamental frequency independently vetted to be 30 Hz towed and 0.1 Hz deployed [17]. Modal analysis was thus constrained to the different modules and the robotic arm, which is a scaled down version based on the Canadarm2.

In the Figure 15 and 16, the modal analyses for the first modes of the various bodies are presented. Displacements magnitudes are meaningless as the forcing functions are arbitrary in amplitude. Mode shapes can be determined by the proportionality of the displacements with respect to each other. The base module has a fundamental frequency of 160.12 Hz with a shape that collapse around the solar array articulation hubs. The propulsion module has a fundamental frequency of 711.91 Hz in a Bessel mode shape, and the thrusters themselves vibrate in their foundations with a fundamental frequency of 126.05 Hz.

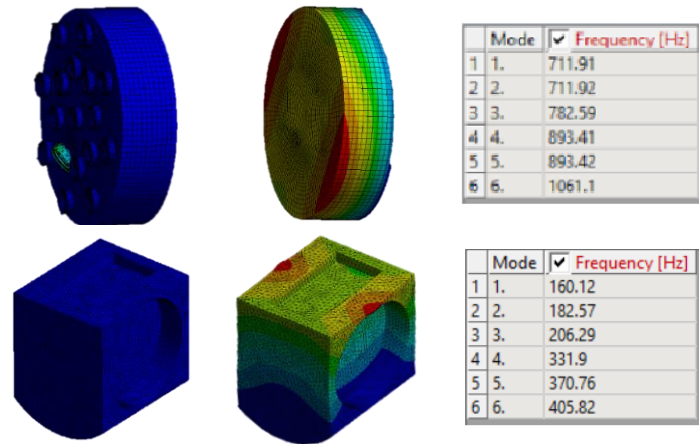


**Figure 15.** Modal Analysis of Base Structure and Propulsion Module

The robotic arm has the lowest fundamental frequency due to its long slender form. The analysis was performed on the arm in its stowed for launch configuration. Four modes with frequencies all around the same were detected, all of which demonstrate some articulation of the booms. These were at 3.82 Hz, 3.90 Hz, 4.60 Hz, and 4.68 Hz.

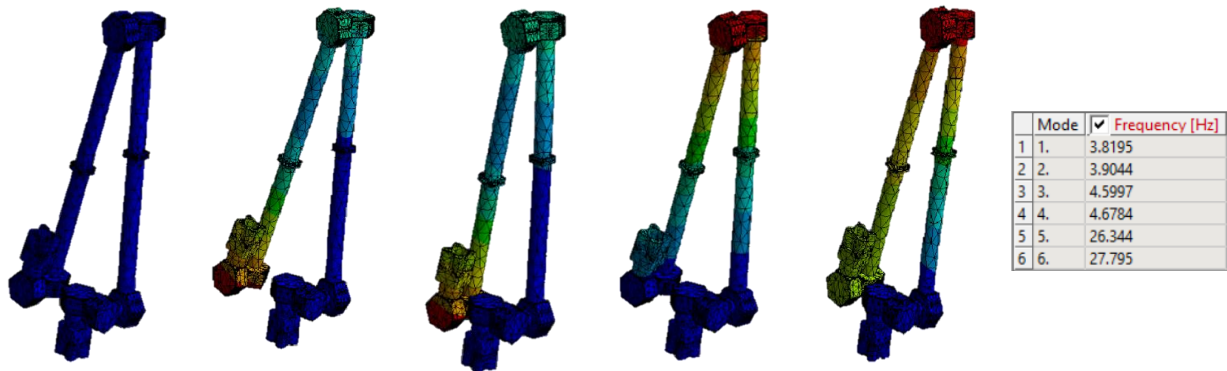


**Figure 16.** Modal Analysis of Robotic Arm

### IV.III Assembly Location and Orbits

#### Schedule of Launch

The payloads will be sent up on 3 different launches using the SpaceX Falcon 9 into LEO and assembled in space. There will be one launch each day for 3 days that will be launched at the inclination that matches the latitude of Kennedy Space Center (KSC) in order to give the most efficient launch into space. The latitude of KSC is 28.5°, which is also the Falcon 9’s minimum value of their inclination range. Launching once each day, the Earth will be in the same position with respect to the inertial orbit, allowing there to be one launch per day for 3 days.

The Falcon 9 will place the payloads into LEO with a perigee of 200 km and an apogee of 360 km. The orbital period is 1.5 hours, which allows the payload to complete 16 orbits in the 24-hour span before the next launch. Ideally, the two payloads would meet up with one another in near proximity in order to complete the assembly process. Once all the payloads are in space, they will be in the same orbit but all at slightly different positions in that orbit. From there, 2 of the payloads will do orbit phasing to either slow down or speed up to the other satellites using RCS thrusters that are on the payloads.

### Trajectory and Mission Design

A detailed trajectory design and optimization was considered out of scope for the details of this project, however a baseline trajectory design was developed to get initial mass estimates for fuel that would be required for the electric propulsion system. As a baseline study of the delta-V requirement, a Hohmann Transfer between a circular parking orbit at the mean height of the ISS to the first Lagrange Point (L1) of the Earth-Moon system is provided. The altitude of the ISS is approximately 404.85 km, and L1 is 326100 km from the center of the Earth. Equation 1 gives the energy of any orbit,  $\mu$  is the gravitational parameter,  $V$  is the velocity, and  $a$  is the semi-major axis.

$$\text{Eq. 1} \quad \mathcal{E} = -\frac{\mu}{2a} = \frac{V^2}{2} - \frac{\mu}{r}$$

The velocity of the LEO parking orbit is:

$$v_1 = \sqrt{\frac{\mu}{r_1}} = \sqrt{\frac{3.986004419E14 \text{ m}^3/\text{s}^2}{7135850 \text{ m}}} = \mathbf{7.473878 \text{ km/s}}$$

The orbital energy of the transfer orbit is:

$$\mathcal{E}_t = -\frac{\mu}{2a} = -\frac{\mu}{r_1 + r_2} = -\frac{3.986004419E14 \frac{\text{m}^3}{\text{s}^2}}{7135850 \text{ m} + 326100000 \text{ m}} = \mathbf{-1.19615114E6 \text{ m}^2/\text{s}^2}$$

Rearranging Equation 1, the velocities necessary at the perigee and apogee of the transfer are given as:

$$v_{t1} = \sqrt{2 \left[ \frac{\mu}{r_1} + \mathcal{E}_t \right]} = \sqrt{2 \left[ \frac{3.986004419E14 \text{ m}^3/\text{s}^2}{7135850 \text{ m}} - 1.19615114E6 \text{ m}^2/\text{s}^2 \right]} = \mathbf{10.455880 \text{ km/s}}$$

$$v_{t2} = \sqrt{2 \left[ \frac{\mu}{r_2} + \mathcal{E}_t \right]} = \sqrt{2 \left[ \frac{3.986004419E14 \text{ m}^3/\text{s}^2}{326100000 \text{ m}} - 1.19615114E6 \text{ m}^2/\text{s}^2 \right]} = \mathbf{0.228800 \text{ km/s}}$$

Finally, the velocity of the final circular orbit at L1 is given as:

$$v_2 = \sqrt{\frac{\mu}{r_2}} = \sqrt{\frac{3.986004419E14 \text{ m}^3/\text{s}^2}{326100000 \text{ m}}} = \mathbf{1.105588 \text{ km/s}}$$

The total delta V and the time of flight (half the period of the elliptical transfer orbit) are shown below:

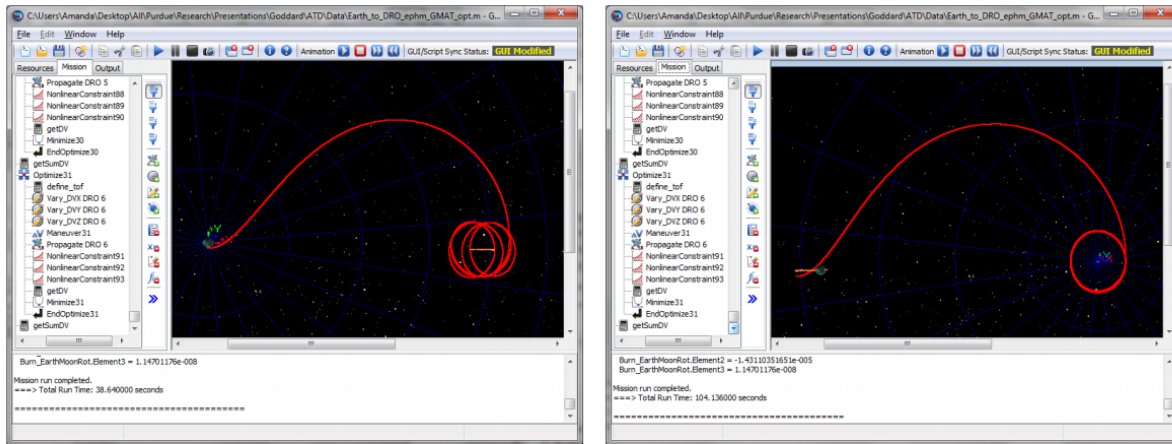
$$\Delta v = v_{t1} - v_1 + v_2 - v_{t2} = \mathbf{3.85879 \text{ km/s}}$$

$$TOF = \pi \sqrt{\frac{a_t^3}{\mu}} = \pi \sqrt{\frac{(166617925 \text{ m})^3}{3.986004419E14 \text{ m}^3/\text{s}^2}} = \mathbf{3.917 \text{ days}}$$

The General Mission Analysis Tool (GMAT) is an open-source space mission design tool developed at NASA Goddard Space Flight Center to analyze the mission specifics of going from LEO to LDRO using electric propulsion. The main purpose this tool used for this mission design was to develop an estimate of time of flight from LEO to LDRO and back. The specifics of the DRO insertion at L1 used GMAT, in order to solve the problem. In order to get into DRO after the arrival in the vicinity of L1 the spacecraft is then placed into an L1 Lyapunov orbit, and then after the orbit grows in size, it is inserted into the desired DRO. Due to time constraints, a proper trajectory model of going from LEO to LDRO could not be developed. An attempt of using GMAT for the mission can be seen in Figure 17. The model is very close to being

complete, as previously mentioned this was out of the focus of the project but is future work to optimize the mission design.

Thankfully, looking through literature a GMAT model has been developed that goes from LEO to LDRO that shows the feasibility of using GMAT to complete the mission design. However, this GMAT model does not include an electric propulsion subsystem. This GMAT model can be seen in Figure 18. [13]



(a) Earth-centered rotating view

(b) Moon-centered rotating view

**Figure 19.** Converged Transfer from LEO to LDRO

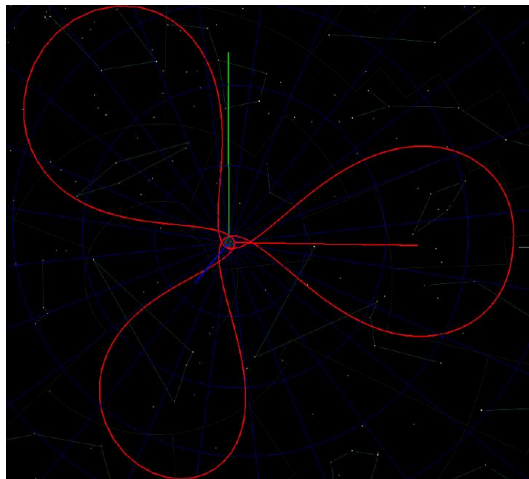


**Figure 17.** Trajectory From LEO to Moon Flyby using L1

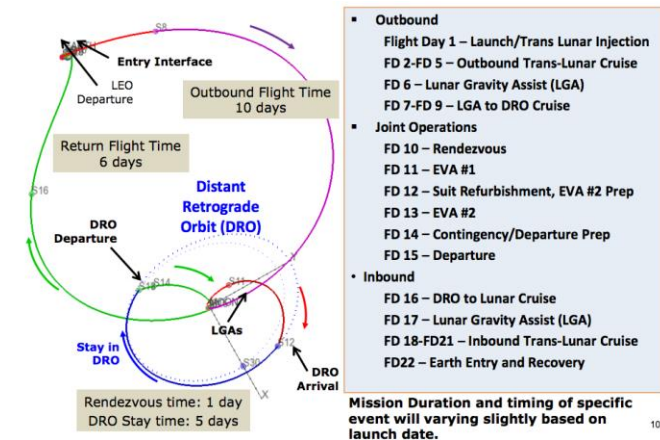


**Figure 18.** Nominal Mission Summary

NASA’s asteroid redirect mission has been able to provide an initial estimate for the time of flight from LEO to LDRO and back. Using a 40 kW SEP system, the time of flight is approximately 22 days from LEO to LDRO and back. [14] The mission plan is shown in Figure 19. A 40 kW SEP is significantly smaller than the 200 kW design that is proposed in this paper, which makes it very feasible for a 200 kW SEP system to complete a LEO to LDRO to LEO orbit on a similar time frame of 22 days that is presented below.

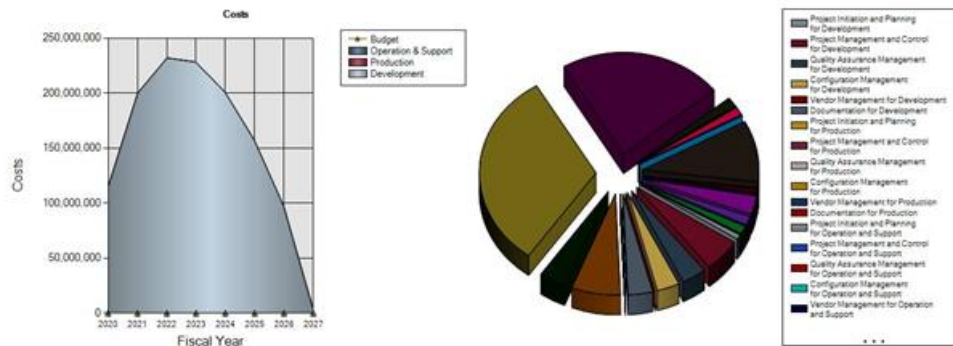
Future work regarding trajectory and mission design include getting an accurate model of our mission working in the GMAT workspace in order to get a better time of flight estimation from LEO to LDRO and back. A more detailed description of the ground assembly testing process would like to be developed to ensure assembly success. There is confidence that the assembly process will be successful based off the Orbital Express mission framework, however with more testing done increasing confidence in the design will result.

### IV.IV Ground Testability

#### Assembly Testing

Since the scale of the vehicle is quite large, full-scale assembly testing would be difficult to conduct. To test the assembly process, a scaled-down version of the vehicle will be built with the same hardware and software onboard. Cables will be used to allow the scaled-down vehicle to have 3 degrees of freedom to move around in, similar to being in space. When the spacecraft is given certain commands (i.e. move upward) the cables will lift the vehicle up in with similar dynamics as if it were in zero gravity. This will be done to simulate getting the three different payloads into the same vicinity to begin the docking process of the spacecraft. The umbrella mechanism, robotic arm, and EPM will then be tested to simulate the docking procedure of the spacecraft. With the simplicity of the docking mechanisms and the low scale cost of the scaled-down model it allows for the users to conduct trial and error of the assembly process. This will save a large amount of money and stress since there won't be any concern of breaking the spacecraft but still be able to get an accurate representation of the assembly process.

### IV.V Cost



TruePlanning 16.0 was used in order to develop a cost estimate for the development and production of our SEP tug. The start of the project is slated for 2020 and to be completed by 2027, with launch in the late 2020's. True planning estimates the costs of parts, labor, development, and production during the entire project length. The estimated total cost of the project is approximately \$1.2 billion. The majority of the costs come from program management and configuration management.

## V. SYSTEMS ANALYSIS OF REQUIREMENTS

### V.I Requirements Modeling

A Systems Modeling Language (SysML) Requirements Diagram was used to breakdown the top-level functional and performance requirements. SysML is widely used by aerospace industries including NASA and Boeing. With a Requirements Diagram, further analysis can later be performed to model the Structural, Behavioral, and Parametric diagrams of the SEP Tug system. An overview of the requirements and respective benchmarks are shown in **Error! Reference source not found.** This is further expanded upon in the SysML Requirements Diagram as shown in Figure 13. From modeling the requirements, the challenges and issues including

**Table 3.** Requirements of SEP System and Benchmarks

Requirement	Benchmark
Assemble SEP tug	Max 60 days
Power generation	Min 200 kW
Withstand acceleration load	Min 0.4G
Fundamental flexible body vibration mode	Min 0.05 Hz
Scalable	Min 500 kW
Design simplicity	High
System mass	Low
Ground testability of assembly process	TRL 5 – 6
System level modularity	High modularity

Technical Readiness Levels (TRLs) of mission-enabling technologies are further identified.

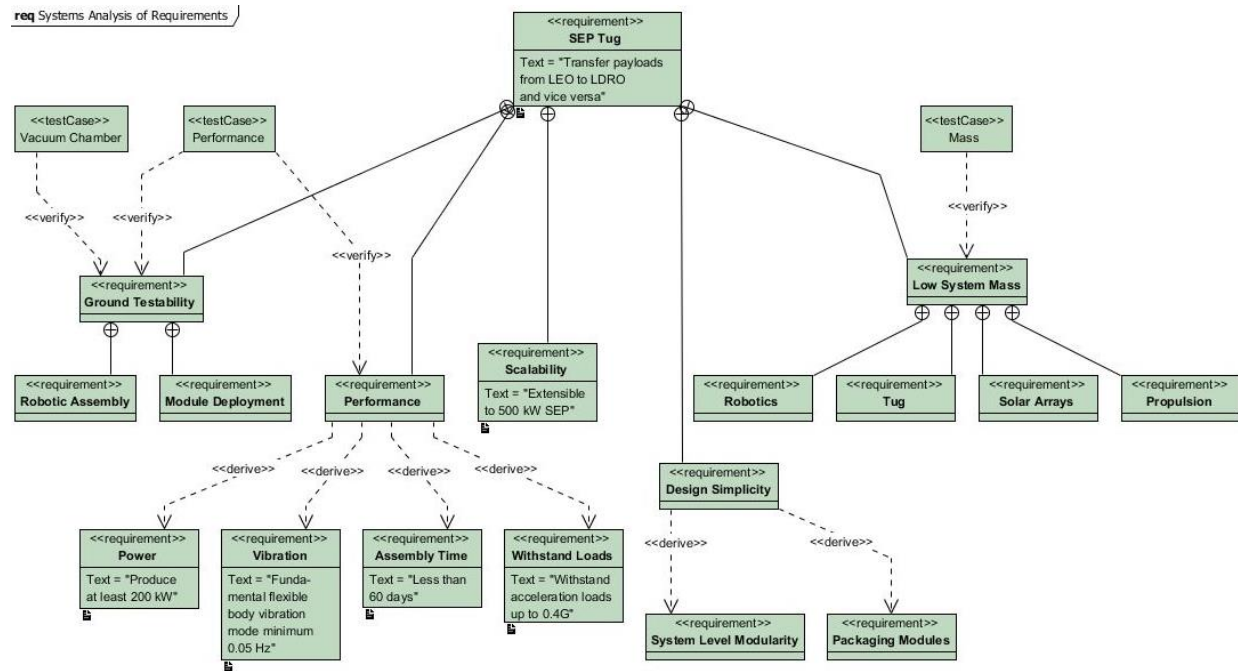


Figure 20. SysML Systems Analysis of Requirements

## II Mission Enabling Technologies

This section provides a review of mission enabling technologies that would allow for future in-space assembly missions. Hamill et al., researched high Technology Readiness Level (TRL) technologies that are key to the future of in-space assembly [17]. The methodology included using a Quality Function Deployment (QFD) to list, weight, and assess technologies. The results of the top 10 important technologies needed to support high priority NASA missions are summarized in Table 4 [17].

Table 4. ISA Technologies Needed to Support High Priority NASA Missions [17]

Rank	Technology	Percentile	TRL
1	simple grasp	100	N/A
2	incorporation of harness-based utilities	64	TRL-5 to TRL-7
3	registration and alignment of components	58	TRL-5 to TRL-7
4	robotic assembly using supervised autonomy	53	TRL-5 to TRL-7
5	buildup from complex stock	48	TRL-5 to TRL-7
6	structurally embedded utilities interfaces	42	TRL-5 to TRL-7
7	proof of joint load capability	36	TRL-5 to TRL-7
8	buildup from simple stock	33	TRL-5 to TRL-7
9	joining by snap-together interfaces	27	TRL-5 to TRL-7
10	joining by combination action	27	TRL-5 to TRL-7

The importance of the technology and rank is subjective; however, this assessment was completed by subject-matter experts in the field of in-space assembly. As noted in the paper, the highest ranked technology is a space-qualified, simple grasp. This supports the design of our SEP Tug which is designed around simplicity.

## APPENDIX

### References

- [1] NIA, and NASA. "2017 BIG Idea Competition." *Big Idea*. N.p., n.d. Web. 30 Nov. 2016.
- [2] "Comparison of Orbital Launch Systems." *Wikipedia*. Wikimedia Foundation, n.d. Web. 30 Nov. 2016.
- [3] Orbital ATK. "UltraFlex™ Solar Array Systems." *Orbital ATK*, n.d. Web. 30 Nov. 2016.
- [4] Schmidt, George R., Michael J. Patterson, and Scott W. Benson. "The NASA Evolutionary Xenon Thruster (NEXT): NASA's Next Step for US Deep Space Propulsion." (2008).
- [5] Dolloff, M. D., and J. Jackson. "Current Status of NASA Evolutionary Xenon Thruster---Commercial (NEXT-C)." *Lunar and Planetary Science Conference*. Vol. 47. 2016.
- [6] Choi, Maria. *Improved hall thruster plume simulation by including magnetic field effects*. Diss. Jet Propulsion Laboratory, 2016.
- [7] Dunbar, Brian. "Canadarm2 and the Mobile Servicing System." *National Aeronautics and Space Administration*, 2013. Web. 30 Nov. 2016.
- [8] Dunbar, Brian. "Space Shuttle Canadarm Robotic Arm Marks 25 Years in Space." National Aeronautics and Space Administration, 2006. Web. 30 Nov. 2016.
- [9] Clark, Stephen. "In-space Satellite Servicing Tests Come to an End." *Spaceflight Now*. N.p., n.d. Web. 30 Nov. 2016.
- [10] Alessandro, Adrienne. "NASA's Restore-L Mission to Refuel Landsat 7, Demonstrate Crosscutting Technologies." *NASA's Goddard Space Flight Center*. N.p., 23 June 2016. Web. 30 Nov. 2016.
- [11] "Electropermanent Magnet." *Wikipedia*. Wikimedia Foundation, n.d. Web. 30 Nov. 2016.
- [12] Bass, Adam, et al. "An Airborne Package Retrieval & Delivery System with Mechanized CG Relocation."
- [13] James Shoemaker ; Melissa Wright; Orbital express space operations architecture program. Proc. SPIE 5419, Spacecraft Platforms and Infrastructure, 57 (August 30, 2004); doi:10.1117/12.544067.
- [14] [https://engineering.purdue.edu/people/kathleen.howell.1/Publications/Conferences/2013\\_AAS\\_Ha aVaqPavHowFol.pdf](https://engineering.purdue.edu/people/kathleen.howell.1/Publications/Conferences/2013_AAS_Ha aVaqPavHowFol.pdf)
- [15] [https://www.nasa.gov/pdf/756678main\\_20130619-NRC\\_Tech\\_Panel\\_Stich.pdf](https://www.nasa.gov/pdf/756678main_20130619-NRC_Tech_Panel_Stich.pdf)
- [16] [http://www.ltas-vis.ulg.ac.be/cmsms/uploads/File/CALVI\\_Students\\_LIEGE\\_2011\\_6.pdf](http://www.ltas-vis.ulg.ac.be/cmsms/uploads/File/CALVI_Students_LIEGE_2011_6.pdf)
- [17] Doris Hamill, Lynn Bowman, David A. Gilman, and Wendel K. Belvin. "High Leverage Technologies for In-Space Assembly of Complex Structures", AIAA SPACE 2016, AIAA SPACE Forum, (AIAA 2016-5397) <http://dx.doi.org/10.2514/6.2016-5397>